

# Thermophysical properties for shock compressed polystyrene

Cong Wang,<sup>1</sup> Xian-Tu He,<sup>1,2</sup> and Ping Zhang<sup>1,2,3,\*</sup>

<sup>1</sup>*LCP, Institute of Applied Physics and Computational Mathematics,  
P.O. Box 8009, Beijing 100088, People's Republic of China*

<sup>2</sup>*Center for Applied Physics and Technology, Peking University, Beijing 100871, People's Republic of China*

<sup>3</sup>*National Institute for Fusion Science, Toki-shi 509-5292, Japan*

We have performed quantum molecular dynamic simulations for warm dense polystyrene at high pressures. The principal Hugoniot up to 790 GPa is derived from wide range equation of states, where contributions from atomic ionizations are semiclassically determined. The optical conductivity is calculated via the Kubo-Greenwood formula, from which the dc electrical conductivity and optical reflectivity are determined. The nonmetal-to-metal transition is identified by gradual decomposition of the polymer. Our results show good agreement with recent high precision laser-driven experiments.

PACS numbers: 82.35.Lr, 51.30.+i, 52.27.Jt, 82.40.Fp, 71.15.Pd

In high energy density ( $E/V \geq 10^{11} \text{J/m}^3$ ) physics (HEDP), pressure-induced response of materials, which can be probed through shock wave experiments [1–4], is of crucial interest for inertial confinement fusion (ICF). Fundamental experiments in typical ICF designs, such as the investigation of hydrodynamic instabilities, have introduced plastic compounds as basic candidates to achieve high gain [5]. Furthermore, in recent fast ignitor experiments, the electrical properties of polymers have been often implicated for the transport of relativistic electron beams in solid targets as compared to conducting materials [6]. Understanding the behavior of polymers at several megabar regime brings better insight into physical processes in ICF.

Some of the ablaters in the indirect-drive mode of National Ignition Facility (NIF), will be made of glow-discharge polymer (GDP) with various levels of germanium doping (Ge-GDP) [7]. Due to the fact that no high pressure data exist for Ge-GDP, polystyrene (CH), which is closest in structure, is considered as a coarse indicator for shock timing simulations of NIF targets involving such ablaters [8]. The absolute equation of states (EOS) of polystyrene along the principal Hugoniot curve has been studied by using gas gun up to 50 GPa [9–12] and high energy laser-driven shock waves up to 4000 GPa [13–15]. High energy dynamic compressions produce the so-called warm dense matter (WDM), where simultaneous dissociations, ionizations, and degenerations make the transition between condensed matter physics to plasma physics. The EOS and the relative properties, such as the Hugoniot curve, are important features in this context. Moreover, electrical properties such as the dielectric function are closely related to the dynamic conductivity, which determines the dc electrical conductivity in the static limit. Then optical reflectance can also be extracted. All these quantities are indispensable in characterizing the unique behavior of shock compressed

polystyrene, especially for high pressures at, or exceeding, 1 Mbar. Recently, the development and application of quantum molecular dynamic (QMD) simulation [16] techniques for WDM are available due to the enormous progress in computer capacity. QMD simulations, where quantum effects and correlations are systematically treated, have conducted highly predictive results to describe WDM.

In the present work, QMD simulations are applied to calculate a broad spectrum of thermophysical properties for shock compressed polystyrene. The self-consistent electronic structure calculation within density functional theory (DFT) yields the charge density distribution in the simulation supercell at every time step. The ion-ion pair correlation function (PCF), which is important for characterizing and identifying phase transitions, can be given by molecular dynamics run. The Hugoniot curve, which is derived from EOS data for a wide region of densities and temperatures, is determined and compared with available experimental and theoretical results. As a starting point, we use the Kubo-Greenwood formula to evaluate the dynamic conductivity  $\sigma(\omega)$ , from which the dc conductivity, the dielectric function  $\epsilon(\omega)$ , and the optical reflectivity can be settled.

We introduce *ab initio* plane wave code VASP [17, 18] to perform QMD simulations. The elements of our calculations consist of a series of volume-fixed supercells including  $N$  atoms, which are repeated periodically throughout the space. By involving Born-Oppenheimer approximation, electrons are quantum mechanically treated through plane-wave, finite-temperature DFT [19], where the electronic states are populated according to Fermi-Dirac distributions. Sufficient occupational bands are included in the overall calculations (the occupational number down to  $10^{-6}$  for electronic states are considered). The exchange-correlation functional is determined by generalized gradient approximation (GGA) with the parametrization of Perdew-Wang 91 [20]. The ion-electron interactions are represented by a projector augmented wave (PAW) pseudopotential [21]. Isokinetic ensemble (NVT) is adopted in the present simulations,

---

\*Corresponding author: zhang\_ping@iapcm.ac.cn

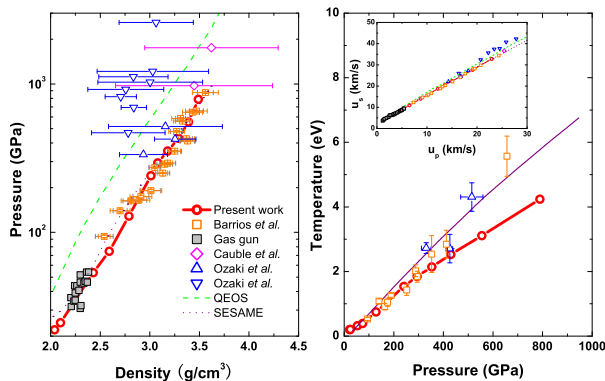


FIG. 1: (Color online) The  $P$ - $V$  (left panel) and  $T$ - $P$  (right panel) Hugoniot curves of shocked polystyrene. Inset is the  $(u_s, u_p)$  diagram. Previous results are also shown for comparison. Experiments: gas-gun results (the gray filled squares); [9–12] absolute measurements on NOVA (magenta diamonds); [13] high energy laser-driven measurements by Ozaki *et al.* [14, 15] (blue upward and downward triangles) and Barrios *et al.* (orange squares). [8] Theories: QEOS and SESAME [26] results are denoted by green dashed line and purple dotted line, respectively.

where the ionic temperature  $T_i$  is controlled by Nosé thermostat [22], and the system is kept in local equilibrium by setting the electron ( $T_e$ ) and ion ( $T_i$ ) temperatures to be equal.

The simulations have been done for 128 atoms (namely, eight  $C_8H_8$  units) in a supercell. A plane-wave cutoff energy of 600.0 eV is selected, so that a convergence of better than 3% is secured. The Brillouin zone is sampled by  $\Gamma$  point and  $3 \times 3 \times 8$  Monkhorst-Pack scheme [23]  $\mathbf{k}$  points in molecular dynamic simulations and electronic structure calculations, respectively, because EOS (conductivity) can only be modified within 5% (15%) for the selection of higher number of  $\mathbf{k}$  points. The densities adopted in our simulations range from 1.05 g/cm<sup>3</sup> to 3.50 g/cm<sup>3</sup> and temperatures between 300 and 50000 K, which highlight the regime of principal Hugoniot. All the dynamic simulations are lasted 6000 steps, and the time steps for the integrations of atomic motion are selected according to different densities (temperatures) [24]. Then, the subsequent 1000 step simulations are used to calculate EOS as running averages.

The nature of high pressure behavior for warm dense polystyrene is dominated by a two-stage transition, that is, dissociations and ionizations. QMD simulations have been demonstrated to be powerful in describing as well as understanding chemical decompositions and electronic excitations of shock compressed materials, namely, the shocked atomic and electronic structures can be effectively treated within QMD. Importantly, however, we should address that the calculated EOS data from direct QMD simulations on shocked polystyrene should be corrected due to the following aspects: (i) At laser-driven temperatures as high as of 5–6 eV ( $\sim 10$  Mbar), the con-

TABLE I: Polystyrene Hugoniot results from QMD simulations.

$\rho$ (g/cm <sup>3</sup> )	$P$ (GPa)	$T$ (eV)	$u_s$ (km/s)	$u_p$ (km/s)
2.04	22.06	0.20	6.59	3.19
2.10	24.61	0.21	6.85	3.42
2.43	53.48	0.32	9.48	5.37
2.59	74.54	0.39	10.93	6.49
2.79	128.56	0.75	14.01	8.74
3.01	240.46	1.54	18.76	12.21
3.08	293.98	1.85	20.60	13.59
3.18	352.98	2.14	22.40	15.01
3.29	429.62	2.53	24.51	16.69
3.39	554.96	3.11	27.67	19.10
3.49	789.07	4.24	32.79	22.92

siderable effect of atomic ionizations on EOS should be appropriately included beyond QMD; (ii) QMD energy consists of kinetic and potential energy (for both ions and electrons), while, the well known zero-point vibration energy (ZPVE), van der Waals energy (VDWE), and so as the demanded energy for phase transitions, which are particularly significant in WDM, are excluded; (iii) The pressure from QMD only describes the interaction contributions, and the ideal part for noninteracting particles are missed. To overcome these obstacles, in our present calculations for polystyrene, ZPVE, which is important for determining the low-pressure internal energy for the reference state along the Hugoniot curve, is simply added onto the QMD output. Condensed matter to plasma transition energy mainly comes from atomic ionization energy, which is also added onto QMD data, and the reference ionization degree is semiclassically determined [25]. VDWE has been treated as small as negligible. As for another important parameter—pressure, contributions from both interacting and noninteracting parts (ions and free electrons, separately) are included in the present EOS data.

High precision EOS data are essential for understanding the electrical and optical properties of polystyrene under extreme conditions. The present EOS have been examined theoretically through the Rankine-Hugoniot (RH) equations, which follow from conservation of mass, momentum, and energy across the front of shock waves. The locus of points in  $(E, P, V)$ -space described by RH equations satisfy the following relations:

$$E_1 - E_0 = \frac{1}{2}(P_1 + P_0)(V - V_0), \quad (1)$$

$$P_1 - P_0 = \rho_0 u_s u_p, \quad (2)$$

$$V_1 = V_0(1 - u_p/u_s), \quad (3)$$

where subscripts 0 and 1 present the initial and shocked state, and  $E$ ,  $P$ ,  $V$  denote internal energy, pressure, volume, respectively. The  $u_s$  and  $u_p$  correspond to the shock

and mass velocities of the material behind the shock front. As the starting point along the Hugoniot, the initial density is  $\rho_0=1.05$  g/cm<sup>3</sup>, and the internal energy is  $E_0=-87.44$  kJ/g at a temperature of 300 K. Compared to the high pressure of shocked states along the Hugoniot, the initial pressure  $P_0$  can be treated approximately as zero. We use smooth functions to fit the internal energy and pressure in terms of temperature at sampled density, and derive Hugoniot point from Eq. 1. The calculated Hugoniot data are listed in Table I.

The principal Hugoniot curve is plotted in Fig. 1, where previous theoretical and experimental results are also shown for comparison. The EOS of polystyrene has been previously probed by gas gun experiments, which have the advantage of high precision, but the pressure hardly exceeds 50 GPa. Recently, high energy laser-driven experiments have detected pressures up to 4000 GPa. Meanwhile, however, large error bars were introduced at above 100 GPa [13, 14], and thus the use of low-precision EOS of the polymer to predict the behavior of NIF Ge-GDP ablator materials provides an unacceptable uncertainty. Then, high precision EOS (up to 1000 GPa) for polystyrene was obtained by using  $\alpha$ -quartz as an impedance-matching (IM) standard [8]. As shown in Fig. 1, previous data by Ozaki *et al.* [14] (IM with an aluminum standard) and Cauble *et al.* [13] (absolute data) show clearly stiffer behavior compared to those results with quartz standard [8, 15] and SESAME model [26]. The possible reason for this stiff behavior is likely due to x-ray preheating of the samples, as has been stated by those authors. Then, thicker pushers and low-Z ablaters were used in the newly measured data from Ozaki *et al.* [15] to reduce pre-heating of the samples. The experiments, where IM with a quartz standard were also used, show results that are closer to those by Barrios *et al.*. In our QMD simulations, we find that direct calculated EOS without corrections mentioned above are only valid in the low pressure ( $P<100$  GPa and  $T<1$  eV) regime, beyond which no Hugoniot points can be found from the pure QMD data. For higher pressures, due to our introduction of corrections to direct QMD results, the calculated principal Hugoniot curve are greatly softened, and the results show good agreements with those experiments where quartz standard was used.

Temperature, as has been focused as one of the most important parameters in experiments, is difficult to be measured because of the uncertainty in determining the optical-intensity loss for ultraviolet part of the spectrum in adiabatic or isentropic shock compressions, especially for the temperature exceeding several eV [27]. QMD simulations can provide efficient predictions for shock temperatures. As has been shown in Fig. 1 (right panel), our calculated Hugoniot temperatures are accordant with experimental results up to 2 eV, and discrepancy emerges at higher temperatures. Beyond 2 eV, the predicted temperatures from both experiments and SESAME model at a given pressure are higher compared to our calculations.

We also examine the structural transition of

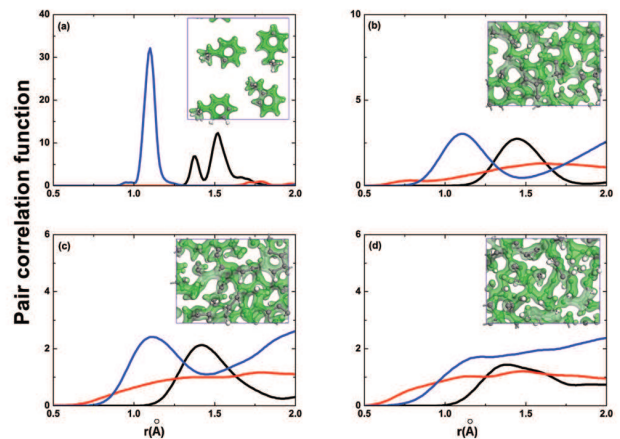


FIG. 2: (Color online) Pair correlation functions for four different points along the principal Hugoniot curve. (a) ~ (d) correspond to the starting point, 53.48 GPa, 74.54GPa, and 128.56 GPa, respectively. C-H, C-C, and H-H bonds are denoted by blue, black, and red lines, respectively. Insets are the sampled atomic structure and charge density distribution at each state (gray balls for carbon and white balls for hydrogen).

polystyrene under shock compressions by using PCF, which is evaluated at equilibrium during the molecular dynamics simulations. Along the Hugoniot, four points of PCF are shown in Fig. 2. At the initial state [see Fig. 2(a)], the ideal condensed polymer phase is indicated by one peak for C-H bond, meanwhile, two peaks ( $\pi$ -type and  $sp^3$ -type) for C-C bond. With the increase of pressure ( $\sim 20$  GPa), phenyl decomposes, which is indicated by that the two C-C peaks merge together (a transverse from  $\pi$  bond to  $sp^2$ ,  $sp^3$  like bond). At this stage diamondlike carbon nanoparticles (with defects) are formed. The present phenomenon agrees well with the behavior of shock compressed benzene [28, 29]. Further increase of pressure produces molecular and atomic hydrogen, which is indicated by the peak in H-H PCF around 0.75 Å [Fig. 2(b)]. Decomposition of hydrocarbons continues until 128 GPa, where PCF shows no obvious evidence for the existence of C-H bond. Whereas, for higher pressures, the PCFs do not show visible difference, and are thus not presented here. SESAME model suggested that the softening behavior of Hugoniot is caused by the chemical decomposition of the polymer at 200 ~ 400 GPa. Whereas, our calculations show that the decomposition pressure lies between 20 and 128 GPa, which is much lower than that of SESAME. Note that the chemical decompositions do not contribute much to the softening behavior, but the ionizations really do.

Having clarified the EOS, let us turn now to study the electrical and optical properties for shocked polystyrene. Based on Kubo-Greenwood formula, the electrical and optical properties can be obtained as described in Ref. [28]. In order to get converged results, 30 independent snapshots, which are selected during one molecular dynamics simulation at given conditions, are picked

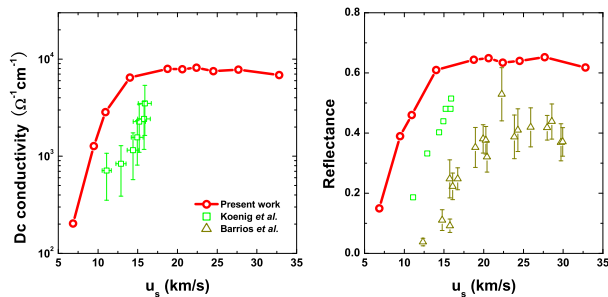


FIG. 3: (Color online) Dc conductivity (left panel) and optical reflectivity at the wavelength of 532 nm (right panel). Previous measurements by Koenig *et al.* (green squares) [30] and Barrios *et al.* (upward triangles) [8] are also plotted.

up to calculate dynamic conductivity as running averages. The dc conductivity  $\sigma_{dc}$ , which follows from the static limit  $\omega \rightarrow 0$  of  $\sigma_1(\omega)$  is then evaluated and plotted in Fig. 3 (left panel) as a function of shock velocity. Initially,  $\sigma_{dc}$  increases rapidly with shock velocity up to 14 km/s (128 GPa) towards the formation of metallic state of polystyrene. Then, one can find from Fig. 3 that  $\sigma_{dc}$  keeps almost invariant and the shock compressed polystyrene maintains its metallic behavior. The onset of metallization ( $\sigma_{dc} > 10^3 \Omega^{-1} \text{cm}^{-1}$ ) is observed at around 10 km/s ( $\sim 50$  GPa), where dissociation of the polymer and formations of hydrogen (molecular and atomic species) govern the characteristics of warm dense polystyrene. We stress here that the nonmetal to metal transition is induced by gradual chemical decompositions and thermal activations of the electronic state, instead of atomic ionization, which is not observed until 128 GPa with respect to the charge density distribution in the QMD simulations. In the same pressure range (20~200 GPa), we observe larger  $\sigma_{dc}$  compared to experimental measurement [30]. This overestimation of  $\sigma_{dc}$  values could be attributed to the use of DFT-based molecular dynamics, which is known to underestimate band gaps in many systems.

Optical reflectance, from which emissivity can be derived, is of great interest in experiment for determin-

ing shock temperature. Along the Hugoniot, we show in Fig. 3 (right panel) the variation of optical reflectance at 532 nm as a function of shock velocity. Optical properties of polystyrene have been experimentally studied by Koenig *et al.* [30] with  $u_s$  of 11~16 km/s (80~170 GPa), and steadily increasing reflectivities reaching values up to  $\sim 50\%$  were observed. The results by Ozaki *et al.* indicated reflectivity from 16% to 42% in  $u_s$  range of 22~27 km/s (300~500 GPa) [15]. Recent experiments by Barrios *et al.* [8] suggested a drastic increase in reflectivity around the Hugoniot pressure of 100 GPa, followed by saturated value of 40% around 250~300 GPa. Discrepancies in reflectivities among experiments have been claimed to be arisen from probe-beam stability or from differences in diagnostic configurations. Along the Hugoniot, our QMD calculations provide the general feature for the optical reflectance—steep increase (from 15% to 60%) followed by saturation (at  $\sim 128$  GPa). The change in optical reflectivity with pressure can be interpreted as the gradual insulator-conductor transition at above 20 GPa, where the atoms strongly fluctuate with neighbors to dense, partially ionized plasma at high pressures above 128 GPa.

In summary, we have carried out QMD simulations to study the thermophysical properties for warm dense polystyrene. The Hugoniot EOS data of polystyrene up to  $\sim 790$  GPa, which is in agreement with dynamic experiments in a wide range of shock conditions, has been evaluated through QMD calculations and corrected by taking into account the atomic ionization. A two-stage (dissociation and ionization) transition governs the characteristic of polystyrene under extreme conditions. Contribution from chemical decomposition demonstrates the steep increase of  $\sigma_{dc}$  and optical reflectance observed at 20~128 GPa. While, soften behavior of the Hugoniot is dominated by atomic ionizations for higher pressure.

This work was supported by NSFC under Grants No. 11005012 and No. 51071032, by the National Basic Security Research Program of China, by the National High-Tech ICF Committee of China, and by the Core University Program.

- 
- [1] M. D. Knudson, and M. P. Desjarlais, *Phys. Rev. Lett.* **103**, 225501 (2009).
- [2] W. J. Nellis, *Rep. Prog. Phys.* **69**, 1479 (2006).
- [3] D. G. Hicks *et al.*, *Phys. Rev. B* **78**, 174102 (2008).
- [4] D. G. Hicks *et al.*, *Phys. Rev. B* **79**, 014112 (2009).
- [5] J. D. Lindl, *Inertial Confinement Fusion: The Quest for Ignition and Energy Gain Using Indirect Drive* (Springer-Verlag, New York, 1998).
- [6] H. Cai *et al.*, *Phys. Rev. Lett.* **102**, 245001 (2009).
- [7] S. W. Haan *et al.*, *Eur. Phys. J. D* **44**, 249 (2007).
- [8] M. A. Barrios *et al.*, *Phys. Plasmas* **17**, 056307 (2010).
- [9] *LASL Shock Hugoniot Data*, Los Alamos Series on Dynamic Material Properties, edited by S. P. Marsh (University of California Press, Berkeley, 1980).
- [10] R. G. McQueen *et al.*, in *High-Velocity Impact Phenomena*, edited by R. Kinslow (Academic, New York, 1970), Chap. VII, Sec. II, p. 293.
- [11] M. Van Thiel, J. Shaner, and E. Salinas, Lawrence Livermore National Laboratory Report No. UCRL-50108, 1977.
- [12] A. V. Bushman, *et al.*, *JETP Lett.* **82**, 895 (1996).
- [13] R. Cauble, *et al.*, *Phys. Plasmas* **4**, 1857 (1997).
- [14] N. Ozaki, *et al.*, *Phys. Plasmas* **12**, 124503 (2005).
- [15] N. Ozaki, *et al.*, *Phys. Plasmas* **16**, 062702 (2009).
- [16] A. Kietzmann, R. Redmer, M. P. Desjarlais, and T. R. Mattsson, *Phys. Rev. Lett.* **101**, 070401 (2008).

- [17] G. Kresse and J. Hafner, Phys. Rev. B **47**, R558 (1993).
- [18] G. Kresse and J. Furthmüller, Phys. Rev. B **54**, 11169 (1996).
- [19] V. Recoules, *et al.*, Phys. Rev. Lett. **102**, 075002 (2009).
- [20] J. P. Perdew, *Electronic Structure of Solids* (Akademie Verlag, Berlin, 1991).
- [21] P. E. Blöchl, Phys. Rev. B **50**, 17953 (1994).
- [22] S. Nosé, J. Chem. Phys. **81**, 511 (1984).
- [23] H. J. Monkhorst and J. D. Pack, Phys. Rev. B **13**, 5188 (1976).
- [24] The time steps have been taken as  $\Delta t = a/20\sqrt{k_B T/m}$ , where  $a = (3/4\pi n_i)^{1/3}$  is the ionic sphere radius ( $n_i$  is the ionic number density),  $k_B T$  presents the kinetic energy, and  $m$  is the ionic mass.
- [25] C. Wang, X. T. He, and P. Zhang, J. Appl. Phys. **108**, 044909 (2010).
- [26] S. P. Lyon and J. D. Johnson, Los Alamos National Laboratory Report No. LA-CP-98-100, 1998.
- [27] Q. F. Chen, private communication.
- [28] C. Wang and P. Zhang, J. Appl. Phys. **107**, 083502 (2010).
- [29] W. J. Nellis, D. C. Hamilton, and A. C. Mitchell, J. Chem. Phys. **115**, 1015 (2001).
- [30] M. Koenig, *et al.*, Phys. Plasmas **10**, 3026 (2003).